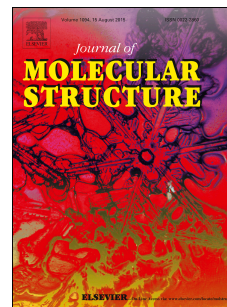


Accepted Manuscript

Synthesis, vibrational, electrostatic potential and NMR studies of (E and Z) 1-(4-chloro-3-nitrophenyl)-3-(2-methoxyphenyl)triaz-1-ene: Combined experimental and DFT approaches

Mohammad Kazem Rofouei, Reza Soleymani, Abolfazl Aghaei, Mahmoud Mirzaei



PII: S0022-2860(16)30639-1

DOI: [10.1016/j.molstruc.2016.06.053](https://doi.org/10.1016/j.molstruc.2016.06.053)

Reference: MOLSTR 22672

To appear in: *Journal of Molecular Structure*

Received Date: 24 February 2016

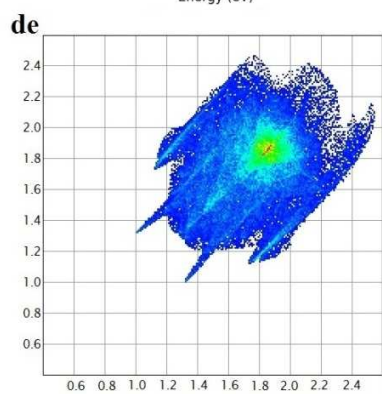
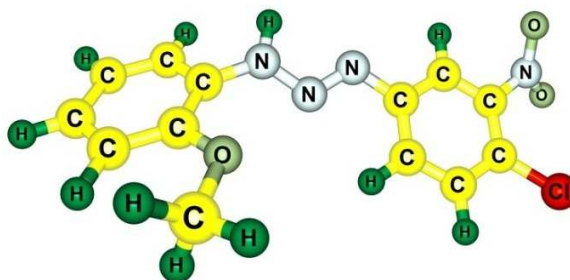
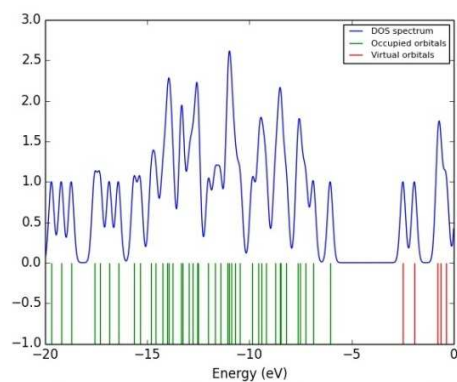
Revised Date: 20 June 2016

Accepted Date: 20 June 2016

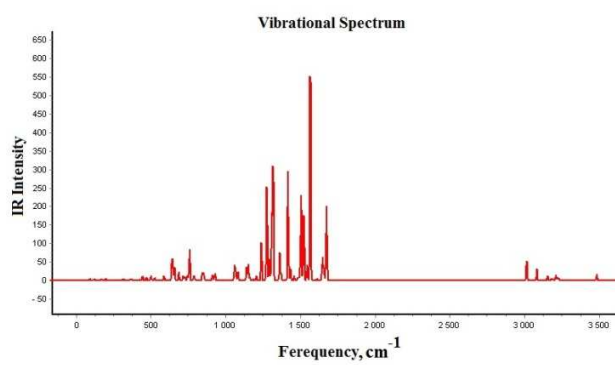
Please cite this article as: M.K. Rofouei, R. Soleymani, A. Aghaei, M. Mirzaei, Synthesis, vibrational, electrostatic potential and NMR studies of (E and Z) 1-(4-chloro-3-nitrophenyl)-3-(2-methoxyphenyl)triaz-1-ene: Combined experimental and DFT approaches, *Journal of Molecular Structure* (2016), doi: 10.1016/j.molstruc.2016.06.053.

This is a PDF file of an unedited manuscript that has been accepted for publication. As a service to our customers we are providing this early version of the manuscript. The manuscript will undergo copyediting, typesetting, and review of the resulting proof before it is published in its final form. Please note that during the production process errors may be discovered which could affect the content, and all legal disclaimers that apply to the journal pertain.

Graphical Abstract (Pictogram)



di



Synthesis, vibrational, electrostatic potential and NMR studies of (E and Z)1-(4-chloro-3-nitrophenyl)-3-(2-methoxyphenyl)triaz-1-ene: Combined experimental and DFT approaches

Mohammad Kazem Rofouei ¹, Reza Soleymani ^{2,*}, Abolfazl Aghaei ³ and Mahmoud Mirzaei ⁴

¹*Faculty of Chemistry, Kharazmi University, Tehran, Iran.*

²*Young Researchers and Elite Club, Shahre-Rey Branch, Islamic Azad University, Tehran, Iran.*

³*Faculty of Chemistry, Tarbiat Moallem University, Tehran, Iran.*

⁴*Bioinformatics Research Center, School of Pharmacy and Pharmaceutical Sciences, Isfahan University of Medical Sciences, Isfahan, Iran.*

* *Corresponding author e-mail address: reza.soleymani@hotmail.com*

Tel: +98 2633350468- Mob: +98 9123782899

Abstract

Using new experimental methods, 1-(4-chloro-3-nitrophenyl)-3-(2-methoxyphenyl) triaz-1-ene, (CNPMP) structure was synthesized in the laboratory. The structure has two E and Z conformational states that E is a more stable state than the Z. After synthesis of the structure, crystallization process was carried out and its chemical properties were investigated using experimental and theoretical methods. The structure has orthorhombic crystal system with space group equal to Pbcn and its unit cell parameters comprise a= 7.0723 (9), b= 7.5333 (9), and c= 13.7138 (15). To further study and identify the structure, in addition to X-Ray diffraction, NMR and FT-IR analyses were also done on the structure. Then, the structure was discussed and studied using density functional theory (DFT) at the theory level B3LYP, B3PW91 and PBE/PBE. The structural and thermodynamic parameters, electrostatic potential, corresponding Hirshfeld surface, electrophilicity (ω), chemical potential (μ), chemical hardness (η) and max amount of electronic charge transfer (ΔN_{max}) were examined for this structure. The results showed that the experimental and theoretical results were very consistent.

Keywords: Synthesis, DFT, Single crystal, Electrophilicity.

1. Introduction

Triazenes are colorful compounds with strong bad smell that normally exist as gases. The compounds also have density and boiling point higher than diazene compounds. These compounds have unsaturated molecular formula $R^1 R^2 N=N-NR^3$ consisting of three nitrogen atoms and three substituted groups. [1] Since the substituted group can be consisted of hydrogen, halogen atoms as well as cyclic compounds, it makes up lots of derivatives. Triazenes have many applications and properties. [2-4] Derivatives of these compounds can be used as various drugs like anti-cancers. [5] However, many derivatives of these compounds are used in paint industry as color indicators. [6] Due to strong electron transport $\pi-\pi^*$, group $N=N-N$ can act as ligands for various metals and make up complex with the metals. [7, 8] One method of producing triazenes is the spontaneous decomposition of Tetrazenes. In this study, it is tried to show a different and modern method for synthesizing these compounds. Triazene compounds have been used for the preparation of several sensors for determination of heavy metals, [9, 10] and also used in solid-phase extraction. [11, 12] They have been studied for their anorectic activity and potency against specific tumor cell lines, [13–17] as well as they have been applied as protecting groups in natural product synthesis [18, 19] or used to form heterocycles. [20, 21] Various compounds have been prepared from these compounds, because of linkage ability of them to carbonic nano tubes that have important abilities especially in man's body metabolism. [22] A kind of these compounds applied in agronomy chemistry for insecticides and weeds synthesis. However, they have been used in pigments synthesis. [23, 24]

HOMO and LUMO are two parameters that can be calculated through density functional theory (DFT). Through these two parameters, we can calculate and examine the electrophilicity values, chemical hardness, chemical potential and the maximum amount of electronic charge

transferred. [25-27] Electrophilicity is in fact a factor to demonstrate the reactivity for organic and inorganic compounds and it is also evaluated and reported for many systems. In fact, high chemical potential and low chemical hardness indicates a system with good electrophone species. Electrophilicity values are different for various compounds based on HOMO and LUMO and accordingly the structure performance in chemical reactions will be different.

Another parameter to be measured is electrostatic potential. In fact the map presented by which shows the charge distribution in the chemical structure. This is available as a three-dimensional map that is composed of red color showing the relative frequency of number of electrons and blue representing the relative lack of electron. [27-28] Once examined the distribution of electrons in the structure, the structure performance in various reactions can be predicted. Usually, yellow and green represent the relative average values of the electrostatic potential. The electrostatic potential is directly related to electronegativity values and the electronegativity difference is a determinate key in the nature of chemical bonding. Hirshfeld surface is a parameter showing the distribution of electron and the electron density in a crystal structure and to obtain it, crystal structure file (CIF) should be available. In fact, it is constructed by partitioning space in the crystal into regions where the electron distribution of a sum of spherical atoms for the molecule dominates the corresponding sum over the crystal. Surface properties are displayed with two parameters d_e and d_i . In fact, we can obtain information on the environment around the crystal structure in the unit cell using this map. d_e is the distance from the Hirshfeld surface to the nearest nucleus outside the surface. d_i is the corresponding distance to the nearest nucleus inside the surface. [29, 30]

2. Experimental details

2.1. General method

All chemicals were of analytical grade and were used as commercially obtained without further purification. ^1H NMR and ^{13}C NMR spectra were recorded on BrukerAvance 300 MHz spectrometer in DMSO solvents, and all chemical shifts were reported in δ unit downfield from Tetramethylsilane (TMS). FT-IR spectra were recorded using Perkin–Elmer RXI spectrometer using KBr disks. Elemental analysis was carried out using a Perkin–Elmer 2,400(II) CHNS/O analyzer.

2.2. Synthesis

The synthetic route is shown in scheme 1. The 0.01 mol (1.72 g) of 4-Chloro-3-nitroaniline was dissolved in 200 mL of acidic solution (6N HCl, $d=1.18$ Kg/L), and the solution was cooled to 0 °C. It was slowly diazotized within 5 min by adding 0.01mol (0.69 g) of sodium nitrite in 10 mL of water under vigorous stirring. After further stirring for 10 min, 0.01mol (1.10 g) of ortho Anisidine in 5 mL methanol was slowly added to the resulting solution under stirring for a period of 10 min. The mixture was maintained at pH 7–8 by adding appropriate amount of aqueous sodium acetate and stirred at room temperature for half an hour. The mixture was filtered out, washed with cold water, and dried in vacuum overnight at room temperature. The brown product (Yield 90%) was dissolved in 30 ml pure acetonitrile (stored in a freezer). Needle like crystals was obtained by slow evaporation of the solvent in a week. ^1H -NMR (300 MHz, DMSO- d_6) δ 7.29–7.66 (7H, m, phenyl protons), 12.97 (1H, s, NH), 3.83 (3H, s, methyl). ^{13}C -NMR (300 MHz, DMSO- d_6) δ 55.86, 113.14, 124.52, 125.70, 125.82, 130.80, 131.08, 134.19, 137.48, 138.08, 155.95, 157.26, 159.90. IR (KBr, ν cm^{-1}): 3305.73 (N-H), 3013.56 (C-H, sp^2), 1422.73-1599.31

(C=C), 1027.06 (C-Cl), 1342.93, 1514.79 (N=O), 1256.63 (C-N), 1042.98, 1256.63 (C-O) 1218.94 (N-N). Elemental Anal. Calc. for $C_{15}H_{15}N_3O$ (306.7 g mol^{-1}): C, 50.91; H, 3.61; N, 18.27. Found: C, 50.97; H, 3.24; N, 18.23%.

3. Computational details

For further comparison, the experimental results of the structure were discussed and studied using DFT at three theory levels, B3LYP, B3PW91 and PBEPBE and basic mode 6-311G (d, p). For this purpose, Gaussian 03 was used. [31] To do so, the structure was preliminary designed using Gauss view 03 and subsequently, the structure was optimized. For all calculations, the standard conditions of the gas phase of 1 atmospheric pressure and 298 Kelvin temperature was considered. To do the calculation, Pentium 4 with RAM memory 4 GB and processor 2.4 Giga Hertz core i7 along with the Windows XP has been used. GIAO method was used to calculate the amount of chemical shift in atoms of carbon and hydrogen. For more consistency of experimental and theoretical results, Tetramethylsilane (TMS) standard was considered to calculate the values of chemical shifts. For this purpose, the structure was initially optimized and then the chemical shift values were calculated. Veda 4 was used for evaluation of the vibrational parameters as well as analysis of structure PED. [32] This application will help to examine the vibrational parameters for each bond based on the intensity of the vibration. For consistency of vibrational parameters obtained experimentally with theoretically obtained values, a different scale factor was used. Values considered for scale factors were intended 0.967 for theory B3LYP, 0.963 for B3PW91 and 0.991 for PBEPBE method. [33] Fingerprint plots and corresponding Hirshfield surface coverage were also examined using CrystalExplorer 3.1. [34]

To investigate the placement of the structure in the unit cell, Mercury 3.6 [35] and to assess and calculate the electrostatic potential values determined for different parts of the structure Molekel software were used. [36]

4. Result and discussion

4.1. Description of the crystal structure

1- (4-chloro-3-nitrophenyl)-3-(2-methoxyphenyl)triaz -1-ene structure (CNPMP) was examined using X-Ray diffraction and its crystallography and structural parameters were assessed. This structure has an empirical formula as $C_{13}H_{11}ClN_4O_3$ (Fig 1). The molecular weight is 306.7. The structure has an Orthorhombic and Space Group Pbc_a crystal system. Orthorhombic crystal system is one of the 7 crystal systems known with three vectors in which the three vectors are unequal and all angles are 90 degree. All data obtained from X-Ray diffraction analysis have been reported in Table 1. As Table 1 shows, the unit cell dimensions in the structure are obtained as $a = 7.0723$ (9), $b = 7.5333$ (9), and $c = 13.7138$ (15), respectively. The placement of structure in the unit cell and the formation of hydrogen bonds are shown in Figure 2. The amount of absorption coefficient for the structure is also obtained 0.292 mm^{-1} .

4.2. Geometrical parameters

4.2.1. Bond length

For better study and results, the chemical and structural parameters of the structure were compared with some similar compounds. The reason to choose these compounds is the structural and chemical similarity, crystallography analysis, and theoretical calculations on

the structures. Surveyed structures include ADQF, [37] TBH derivatives, [38] DMPF, [39] DPTF, [40] and BH complexes. [41] The structural parameters were studied using experimental methods, crystallography method and also using density functional theory at three different levels, B3LYP, B3PW91 and PBEPBE. The results have been reported in Table 2. As Table 2 shows, the bond N=N was obtained 1.261 Å using the experimental method, and 1.262, 1.260 and 1.282 Å, respectively using B3LYP, B3PW91 and PBEPBE methods. However, for N-N bond using experimental method, it is obtained 1.328 Å and using B3LYP, B3PW91 and PBEPBE methods, 1.324, 1.318 and 1.328 Å, respectively. Results of other bonds' length suggest the top consistency of the theoretical and experimental results. As shown in Table 2 and supplementary dataS1, the experimental and theoretical results are highly consistent. In the structure TBH derivatives, [38] the N-N bond length was reported 1.328 to 1.387 Å using experimental methods and 1.315 to 1.351 Å using theoretical method. However, N-N bond in the structure of BH complexes were obtained 1.310 to 1.384 Å using the theory method that is highly consistent with results obtained for the CNPMPT. [41] Also, if the bonds C-C, C = C and C-N in CNPMPT structure are compared with other structures, you will see that the results are highly consistent with similar structures. [37-41]

4.2.2. Bond angle and dihedral angle

The results of the bond and planar angles in CNPMPT structure are quite close to the results obtained for the length of bonds with similar structures. The obtained experimental and theoretical results are also quite close to each other. For example, the experimental results for N22-N21-N20 was 112.4 degrees that based on B3LYP, B3PW91 and PBEPBE methods, it is obtained 112.5, 112.3 and 111 degrees, respectively. Also, the bond angle for N21-N20-C3 was obtained 121.2 degrees using the experimental results and 123.8, 123.9 and 126.9 degrees,

respectively using theory methods based on B3LYP, B3PW91 and PBEPBE methods. Of course, depending on the type of substitution orientation and conformational state used by the structure, the bond and planar angles will have different values. Space congestion in the substituent groups will affect the results.

4.3. Vibrational assignments

Comparing the infrared spectrum of two substances, they are believed to be similar, one can discover whether they really are equal or not. If all the adsorptions in the spectrum of two molecules are coincided, then almost certainly the two are the same. The second use of the infrared spectrum that is more important than the first is that it gives information about the structure of a molecule. Adsorptions associated with each bond can be found in a small part of infrared vibrational area. CNPMPT structure contains 32 atoms and 90 normal vibration parameters. FT-IR analysis on the structure were obtained using experimental and theoretical methods (Fig 3). To calculate the vibrating parameters of CNPMPT structure, DFT method at three levels of theory B3LYP, B3PW91 and PBEPBE and the basic state 6-311G (d, p) was used. For more consistent results with experimental results, the conversion factor 0.967, 0.963 and 0.991 were used respectively. [33] As shown in Table 3, the experimental and theoretical results are highly consistent. Comparing experimental method with DFT method at B3LYP theory level showed linear equation $Y = 1.0165x - 15.643$ with $R^2 = 0.9997$, comparison with the theoretical level B3PW91 showed linear equation $Y = 1.0171x - 14.58$ with $R^2 = 0.9997$ and then comparison with theoretical level PBEPBE showed linear equation $Y = 1.0171x - 22.004$ with $R^2 = 0.9995$ (Supplementary dataS2.).

4.3.1. C-H vibrations

C-H vibration parameter is entirely dependent on the type of hybridization. CH vibration parameter with SP^3 hybridization appears below 3000 and with SP^2 hybridization in the range of 3100 and with SP hybridization upper than 3200. Stretching vibration usually appear in the range of 2850 to 3200. Depending on the type of hybridization, bending vibrations are expected to be appeared in the range of 1000 to 1300 cm^{-1} . But for CNPMPT structure, C-H stretching vibration appeared in the range of 3090, 3013, 2977, 2944 and 2840 cm^{-1} with various intensities using the experimental FT-IR. But using DFT method at B3LYP theory level, CH stretching vibrations appear in the range of 2907 to 3117 cm^{-1} and at B3PW91 theory level in the range of 2902 to 3111 cm^{-1} and for PBEPBE theory level in the range of 2912 to 3123 cm^{-1} . But comparing CNPMPT structure with other structures shows similar results from the vibration amplitude. For structure DPTF was observed in the range of 2978 to 3212 cm^{-1} using the experimental method, in the range of 3155 to 3281 cm^{-1} using DFT at B3LYP theory level [40]. In the BH structure, [41] complexes appear in the range of 2700 to 3180 cm^{-1} using experimental methods of vibration amplitude based on the type of vibration and using theory in the range of 2800 to 3012. However, in the structure [37] ADQF, C-H stretching vibration amplitude was observed in the range of 2916 cm^{-1} using the experimental method and in the range of 2854 to 3063 cm^{-1} using theoretical method. But bending vibration C-H using the experimental method was observed in the range of 1145 and 1157 and through DFT method at three levels of theory B3LYP, B3PW91 and PBEPBE in the range of 1127 to 1165 and 1120 to 1160 cm^{-1} as well as 1115 to 1145 cm^{-1} . The results obtained for C-H bending vibration in CNPMPT structure are consistent with the results obtained for other compounds. [37-41]

4.3.2. NO_2 vibrations

The experimental results obtained for CNPMPT structure shows the symmetric stretching vibration of NO_2 within the range of 1599, 1569, 1523 cm^{-1} and asymmetric stretching vibration in the range of 1342 cm^{-1} . However, theoretical calculations using DFT method at three levels of theory B3LYP, B3PW91 and PBEPBE show symmetric and asymmetric stretching vibration in different areas. At B3LYP level, it shows the asymmetric stretching vibration in the range of 1339 cm^{-1} and symmetric stretching vibration in districts 1540, 1567 and 1591 cm^{-1} . At B3PW91 level, the symmetric stretching vibration is shown in the range of 1550, 1582 and 1612 cm^{-1} as well as asymmetric stretching vibration in the range of 1364 cm^{-1} . PBEPBE also shows symmetric stretching vibration in the area 1528, 1549 and 1583 cm^{-1} and asymmetric stretching vibration in the range of 1351 cm^{-1} . NO_2 group gives two strong bonds in the infrared spectrum. In these compounds, asymmetric stretching vibration is appeared in 1500 to 1600 cm^{-1} and asymmetric stretching vibration in the range of 1300 to 1400 cm^{-1} , because of the resonance in the functional group NO_2 .

4.3.3. C-C and C=C vibrations

C-C and C=C stretching vibration is within the circular structure. Using the experimental approach, the vibration amplitude for the structure CNPMPT is observed in 1523 cm^{-1} and using the theory method, the vibration amplitude using DFT at three theoretical level B3LYP, B3PW91 and PBEPBE was in the 1410-1591, 1404-1612 and 1394-1583 cm^{-1} , respectively. Tension ring adsorptions are usually appeared in pairs in the range of 1575 to 1600 cm^{-1} , and Everton/Hybrid strips are expected to be appeared in the range of 1600 to 2000 cm^{-1} . However, the amplitude of stretching and bending vibrations changes depending on the type and number of

substitutions. In similar structures such as DPTF, [40] the amplitude of stretching vibrations of C-C appear from 1413 to 1492 cm^{-1} , while appears in the region of 1482 to 1550 cm^{-1} by using DFT method. In TBH derivatives, [38] using the theory of revealed that vibration amplitude of C=C and C-C bonds, which have resonance, appear from 1251 to 1613 cm^{-1} , which experimentally appeared in the range of 1239 to 1621 cm^{-1} . Moreover, in DMPF structure, [39] the experimental results indicated that the amplitude of stretching vibration of C-C appear in the region of 1516, 1323, and 1300 cm^{-1} . The theoretical results for this structure match perfectly with experimental results. The bending vibration of C-C-C group appear in region less than 1050 cm^{-1} . In CNPMPT structure, the bending vibration of C-C-C group appear in the regions of 673, 747, 783, and 1027 cm^{-1} using experimental method. The theoretical results using DFT method also shows the bending vibration of C-C-C in three regions of 568-1099, 567-1027, and 564-1011 cm^{-1} in three theoretical levels of B3LYP, B3PW91, and PBEPBE, respectively. The amplitude of bending vibration were also in the same range for similar components. [37-41]

4.3.4. N-H vibrations

In DMPF structure, N-H stretching vibration was in the range of 3301 cm^{-1} by experimental method, while appeared in the range of 3448 and 3436 cm^{-1} using theoretical method. In BH complexes, [41] the N-H stretching vibration was in the range of 3428 to 3691 cm^{-1} by experimental method, while appeared in the range of 3579 and 3583 cm^{-1} using theoretical method. In ADQF structure, [37] it was in the range of 3173 and 3367 cm^{-1} by experimental method, and in the region of 3367 to 3503 cm^{-1} by theoretical method. The first and second types of amines and also amides have the stretching and bending vibrations of NH groups. The amplitude of stretching vibrations of this group is between 3100 and 3500 cm^{-1} with medium to high peak intensity, and its bending vibration is in the range of 1500 to 1700 cm^{-1} . But in

CNPMPT structure, the amplitude of N-H stretching vibration is about 3305 cm^{-1} by experimental method, while appears in 3351 , 3353 , and 3290 cm^{-1} by using DFT method in three theoretical level of B3LYP, B3PW91, and PBEPBE, respectively. The bending vibration for CNPMPT structure was in the range of 1476 and 1514 cm^{-1} by experimental method, while appeared in three regions of 1498 - 1500 , 1488 - 1508 , and 1480 - 1500 cm^{-1} by using DFT method in three theoretical level of B3LYP, B3PW91, and PBEPBE, respectively. Investigating similar structures also showed N-H group bending vibrations in the range of 1530 to 1670 cm^{-1} .

4.3.5. C-N vibrations

In ADQF structure, [37] C-N stretching vibration appeared in the region of 1208 cm^{-1} by experimental results, and in the range of 1208 and 1296 cm^{-1} by theoretical method. The stretching vibration of C=N was appeared in the region of 1479 cm^{-1} by theoretical method. [41] In TBH derivatives, [38] the stretching vibration of C=N was in the range of 1179 to 1571 cm^{-1} by experimental method, and was appeared in the range of 1126 to 1542 cm^{-1} by theoretical method. However, this range of changes are due to presence of resonance and aromatic mode. In amine groups and aromatic amines, the stretching vibration of aromatic C-N appears in the range of 1000 to 1350 cm^{-1} , and the stretching vibration of C=N appears in the range of 1500 to 1650 cm^{-1} . Moreover, the bending vibration associated with C-N and C=N usually appear in the region of 400 to 800 cm^{-1} with rather medium intensities. In CNPMPT structure, there should be no vibration for C=N. but presence of resonance between nitrogen and carbon atoms increases the absorption range of this bond and the rank of bond increases from 1 to 2 in some cases. In this structure, the stretching vibration of C-N group was in the region of 1218 cm^{-1} by experimental method, while appeared in three levels of 1220 - 1243 , 1227 - 1243 , and 1223 - 1237 cm^{-1} by DFT method in three theoretical level of B3LYP, B3PW91, and PBEPBE, respectively. For C=N

bond, the liberation was also in the region of 1514 cm^{-1} by experimental method, and in three regions of 1500 , 1508 , and 1500 cm^{-1} by DFT method in three theoretical level of B3LYP, B3PW91, and PBEPBE, respectively. As Table 3 indicates, the bending vibration of C-N group also appears in regions less than 750 cm^{-1} .

4.3.6. N=N and N-N vibrations

In BH complexes, [41] the stretching vibration of N=N was in the range of 1056 to 1257 cm^{-1} by experimental method, and in the range of 1045 to 1267 cm^{-1} by theoretical method. The stretching and bending vibrations are usually visible for N-N and N=N bonds in treasons. In CNPMPT structure, the amplitude of N-N bond vibration is in the range of 1218 and 1256 cm^{-1} by experimental method, and in the range of 1184 - 1255 , 1192 - 1259 , and 1183 - 1258 cm^{-1} by DFT method in three theoretical level of B3LYP, B3PW91, and PBEPBE, respectively. The amplitude of vibration for N=N bond is also in the range of 1463 and 1514 cm^{-1} by experimental method, and in the range of 1453 - 1500 , 1449 - 1508 , and 1437 - 1500 cm^{-1} by DFT method in three theoretical level of B3LYP, B3PW91, and PBEPBE, respectively. Furthermore, the amplitude of bending vibration of N-N-N is below 1000 cm^{-1} .

4.3.7. C-O vibrations

The vibration of C-O group in CNPMPT is in the range of 1027 , 1218 , and 1256 cm^{-1} by experimental method, and in the range of 1017 - 1269 , 1020 - 1269 , and 1009 - 1262 cm^{-1} by DFT method in three theoretical level of B3LYP, B3PW91, and PBEPBE, respectively. The methoxy group attached to the aromatic ring includes C-O bond, where two different types of carbon are attached to oxygen. Therefore, the stretching vibration of C-O group is visible in two different regions. It is usually expected that the stretching vibration of C-O appears in the range of 950 to

1300 cm^{-1} . In DMPF structure, [39] the stretching vibration of C-O group is reported in two regions of 1990 and 1213 cm^{-1} by experimental method.

4.3.8. C-Cl vibrations

The stretching vibration of C-Cl in CNPMPT structure was appeared to be in the region of 1027 cm^{-1} by experimental method, and in the range of 1019-1093, 1027-1097, and 1011-1084 1262 cm^{-1} by DFT method in three theoretical level of B3LYP, B3PW91, and PBEPBE, respectively. It has to be noted that aryl chlorines are expected to be appeared in the range of 1100 to 1305 cm^{-1} . The bending movement occurs easier than stretching movement and the constant force coefficient, K, is smaller for it. Moreover, the bonds between atoms with higher weights vibrate in lower frequencies compared to the bonds between atoms with lower weights. The trend of C-H > C-C > C-O > C-Cl > C-Br > C-I is based on increasing vibration frequency.

4.4. NMR spectra

Nuclear magnetic resonance was first discovered in 1946, by Felix Bloch from Stanford University and Edward Purcell from Harvard University, independently. [42] They showed absorption of electromagnetic radiation resulted from transfer of nucleus energy levels occurred in a strong magnetic field. These two physicists achieved the Nobel Prize of 1952 for their work. [43] In the first five years after discovery of nuclear magnetic resonance method, chemists found out that the molecular environment of objects affects the absorption of radiation by nucleons in presence of a magnetic field, and this effect could be attributed to the molecular structure. The development of nuclear magnetic resonance spectroscopy method was remarkable since then, and this method has had a significant effect on development of organic chemistry, inorganic chemistry and biochemistry. For further characterization of CNPMPT structure, besides FT-IR

investigation, the amounts of chemical shifts for carbon and hydrogen atoms are also discussed by utilizing the experimental and theoretical method of density function (Supplementary dataS3). As the obtained results in tables 4 and supplementary dataS4 show, the results of chemical shift of carbon atoms are highly consistent with each other. However, the results of hydrogen atoms are a little different in some cases which could be attributed to solvent effects on hydrogen atoms in empirical mode. The theoretical calculations are performed in gas phase and the solvent effects are neglected. But the values of chemical shift are different depending on the type of nucleon and chemical environment of atoms. The gauge including atomic orbitals (GIAO) method was used to carry out calculations in three theoretical levels of B3LYP, B3PW91, and PBEPBE. This method is applicable to calculate chemical shifts of many components and gives precise results consistent with chemical shifts obtained experimentally. [43-45] The base mode of 6-311G(d,P) was utilized for all theoretical levels. The results are TMS chemical shifts are used as reference. First, the structure was optimized and the amounts of chemical shift was calculated for different atoms. The consistency is rather high in ^{13}C -NMR results. But there is a high discrepancy between theoretical and experimental results for ^1H -NMR, especially in H19, which is due to solvent effects in experimental results, as mentioned earlier.

4.5. Molecular electronic potential maps

As the electrostatic potential map in Fig. 4 shows, charge distribution is different for different parts of CNPMPT molecule in three theoretical levels of B3LYP, B3PW91, and PBEPBE. The hydrogen atoms in this map have the lowest electrostatic potential, while the oxygen atoms have the highest electrostatic potential. The chlorine atom is also shown in green and is within the middle range of electrostatic potential. The obtained results for three theoretical levels are almost similar. Furthermore, nitrogen atoms belonging to treason group are shown in yellow and almost

have a more negative value compared to chlorine. The electrostatic potential actually represents charge distribution of molecules in three dimensions. This map actually enables one to identify and investigate the charge distribution and atomic charges in different parts of molecules. Predicting the behavior and function of molecules in chemical reactions is also possible via this. In order to compute and present this map, first, the corresponding structure is optimized by utilizing density functional theory, then the electrostatic potential map is calculated and recorded using Molkele software. As shown in Fig. 4, the range of electrostatic potential changes for CNPMPT structure in three theoretical levels of B3LYP, B3PW91, and PBEPBE is -0.0835-0.0553, -0.0864-0.0597, and -0.0818-0.0592, respectively.

4.6. Fingerprint plots and corresponding Hirshfield surface coverage for CNPMPT structure

3D shapes of Hirshfield surface coverage and 2D images of Fingerprint plots showed the share of each atom in molecular interactions. Hydrogen atom had the highest share of 51.5% in Fingerprint plots. On the other hand, nitrogen atoms had the lowest share of 8.1% in Fingerprint plots and molecular interactions. Hirshfield surface analysis actually shows the molecular interactions in 3D. The share of each molecular interactions is shown in Fig. 5.

4.7. Other molecular properties

The thermodynamic parameters, HOMO and LUMO values are discussed and investigated through DFT results in three theoretical levels of B3LYP, B3PW91, and PBEPBE (Table 5). By extracting these values, the electrophilicity, chemical hardness, chemical potential, dipole moment, zero-point vibrational energy, entropy, and heat capacity of this structure is examined and reported. The obtained results indicate the stability of structure in conformational state of E (Supplementary dataS5). Although after conformational drawing of Z for this structure and

optimization, because state E is more stable than state Z, again the optimized structure would choose the conformational state of E with the lower energy level as the spatial interactions are lower in this state. Further comparisons were done using GaussSum software, and DOS Spectrum for all cases is reported in supplementary data S6.

Crystallographic data for structural analysis reported in this paper have been deposited with the Cambridge Crystallographic Data Centre and allocated the deposition number CCDC 1433072. These data can be obtained free of charge via www.ccdc.cam.ac.uk/conts/retrieving.html (or from the Cambridge Crystallographic Data Centre, 12, Union Road, Cambridge CB2 1EZ, UK; Fax: +44 1223 336033, e-mail: deposit@ccdc.cam.ac.uk).

5. Conclusions

CNPMPT structure is unique and has many applications in various chemical, medical, painting, industries etc. This compound is able to form complexes with different metals and can act as a multi-denticity ligand in different complexes. Furthermore, this structure is capable of having specific medicinal or antibacterial properties due to having two conformations of E and Z, which can be investigated by other researchers in the future. This structure is synthesized by a new method, investigated and characterized by FT-IR, Absorbance electron spectrum, $^1\text{H-NMR}$, $^{13}\text{C-NMR}$, and X-ray single crystal diffraction. The theoretical calculations for this structure are discussed in the following using DFT method in three levels of B3LYP, B3PW91, and PBE/PBE. CNPMPT structure has an orthorhombic structure with Pbcn space group and a wavelength of 0.71073. The DFT results in B3LYP theoretical level showed that this structure has a total energy of -882733.1034 KCal/mol. Total entropy of this structure is 146.169 Cal/Mol-Kelvin,

and its heat capacity is 69.157 Cal/Mol-Kelvin. This structure has the ability of forming polymer and can form hydrogen bonds with the atoms in its neighborhood.

Acknowledgements

The authors are indebted to Ms. Esfandyar and Mr. Ehsan Fereyduni, for their interest in this work and many helpful discussions.

References

- [1] D.B. Kimball, M.M. Haley, Triazenes: A versatile tool in organic synthesis. *Angew Chem Int Ed Engl.* 41 (2002) 3338-3351.
- [2] R. Lazny, J. Poplawski, J. Köbberling, D. Enders, S. Bräse, Triazenes: A useful protecting strategy for sensitive secondary amines. *Synlett.* 8 (1999) 1304-1306.
- [3] M. Kazem-Rostami, A. Khazaei, A.R. Moosavi-Zare, M. Bayat, S.Saednia, Novel one-pot synthesis of thiophenols from related triazenes under mild conditions. *Synlett.* 23 (2012) 1893-1896.
- [4] A. Goeminne, P.J. Scammells, S.M. Devine, B.L. Flynn, Richter cyclization and co-cyclization reactions of triazene-masked diazonium ions. *Tetrahedron Lett.* 51 (2010) 6882-6885.
- [5] D. Ionescu, V.Neagu, V. Dobre, I. Niculescu-Duvaz, Potential anticancer agents. XXII. Pharmacological properties of some new triazene derivatives. *Neoplasma.*28 (1981)19-26.
- [6] W.B. Chen, W.X. Ma, X.Y. Xu, Synthesis of 1-(4-antipyrine)-3-(3-nitroaniline)-triazene and its color reaction with Mercury(II). *Adv. Mater. Res.* 455-456 (2012) 895-900.
- [7] H. Tavallali, H. Shafiekhani, M.K. Rofouei, M. Payehghadr, A new triazene ligand immobilized on triacetylcellulose membrane for selective determination of Mercury ion. *J. Braz. Chem. Soc.* 25 (2014) 861-866.
- [8] M.K. Rofouei, M.R. Melardi, M. Barkhi, H.R.K. Ghaydar, Synthesis and crystal structure of Bis[1,3-bis(2-methoxyphenyl)triazene]mercury(II). *Japan Soc. Anal. Chem.* 24 (2008) X81-X82.
- [9] M.B. Gholivand, M. Mohammadi, M. Khodadadian, M.K. Rofouei, Novel platinum(II) selective membrane electrode based on 1,3-bis(2-cyanobenzene)triazene. *Talanta.* 78 (2009) 922-928.

- [10] M.B. Gholivand, M. Mohammadi, M.K. Rofouei, Optical sensor based on 1,3-di(2-methoxyphenyl)triazene for monitoring trace amounts of mercury(II) in water samples. *Mater. Sci. Eng. C* 30 (2010) 847-852.
- [11] M.K. Rofouei, M. Payehghadr, M. Shamsipur, A. Ahmadalinezhad, Solid phase extraction of ultra traces silver(I) using octadecyl silica membrane disks modified by 1,3-bis(2-cyanobenzene) triazene (CBT) ligand prior to determination by flame atomic absorption. *J. Hazard. Mater.*, 168 (2009) 1184-1187.
- [12] M.K. Rofouei, A. Sabouri, A. Ahmadalinezhad, H. Ferdowsi, Solid phase extraction of ultra traces mercury (II) using octadecyl silica membrane disks modified by 1,3-bis(2-ethoxyphenyl)triazene (EPT) ligand and determination by cold vapor atomic absorption spectrometry. *J. Hazard. Mater.* 192 (2011) 1358-1363.
- [13] D.T. Hill, K.G. Stanley, J.E. Williams, B. Love, P.J. Fowler, J.P. McCafferty, E. Macko, C.E. Berkoff, C.B. Ladd, 1,3-Diaryltriazenes: a new class of anorectic agents. *J. Med. Chem.* 26 (1983) 865-869.
- [14] F. Brahim, Z. Rachid, J.P. McNamee, M.A. Alaoui-Jamali, A.M. Tari, B.J. Jean-Claude, Mechanism of action of a novel "combi-triazene" engineered to possess a polar functional group on the alkylating moiety: Evidence for enhancement of potency. *Biochem. Pharmacol.* 70 (2005) 511-519.
- [15] H. Adibi, M. B. Majnooni, A. Mostafaie, K. Mansouri and M. Mohammadi, Synthesis, and in-vitro cytotoxicity studies of a series of triazene derivatives on human cancer cell lines. *Iran. J. Pharm. Res.* 12 (2013) 695-703.
- [16] H.S. Friedman, T. Kerby, H. Calvert, Temozolomide and treatment of malignant glioma. *Clin. Cancer Res.* 6 (2000) 2585-2597.

- [17] S.S. Agarwala, J.M. Kirkwood, Temozolomide, a novel alkylating agent with activity in the central nervous system, may improve the treatment of advanced metastatic melanoma. *Oncologist*, 5 (2000) 144-151.
- [18] K.C. Nicolaou, C.N.C. Boddy, H. Li, A.E. Koumbis, R. Hughes, S. Natarajan, N.F. Jain, J.M. Ramanjulu, S. Bräse, M.E. Solomon, Total synthesis of vancomycin—part 2: Retrosynthetic analysis, synthesis of amino acid building blocks and strategy evaluations. *Chem. Eur. J.* 5 (1999) 2602-2621.
- [19] P. Lazny, M. Sienkiewicz, S. Bräse, Application of triazenes for protection of secondary amines. *Tetrahedron*. 57 (2001) 5825-5832.
- [20] P. Knochel, C.Y. Liu, Preparation of polyfunctional arylmagnesium reagents bearing a triazene moiety. A new carbazole synthesis. *Org. Lett.* 7 (2005) 2543-2546.
- [21] D.B. Kimball, T.J.R. Weakley, R. Herges, M.M. Haley, Deciphering the mechanistic dichotomy in the cyclization of 1-(2-Ethynylphenyl)-3,3-dialkyltriazenes: Competition between pericyclic and pseudocoarctate pathways. *J. Am. Chem. Soc.* 124 (2002) 13463-13473.
- [22] H.A. Dabbagh, A. Teimouri, A. Najafi, R. Shiasi, DFT and ab initio calculations of the vibrational frequencies and visible spectra of triazenes derived from cyclic amines. *Spectrochim. Acta Part A* 67 (2007) 437-443.
- [23] A. Zarei, L. Khazdooz, H. Aghaei, G. Azizi, A.N.Chermahinie, A. R. Hajipour, Synthesis of triazenes by using aryl diazonium silica sulfates under mild conditions. *Dyes and Pigments* 101(2014) 295-302.
- [24] B.A. Iglesias, M. Hörner, H.E. Toma, K. Araki, 5-(1-(4-phenyl)-3-(4-nitrophenyl)triazene)-10,15,20-triphenylporphyrin: a new triazene-porphyrin dye and its spectroelectrochemical properties. *J. Porphyrins Phthalocyan.* 16 (2012) 200-209.

- [25] R.G. Parr, L.V. Szentpály, S. Liu, Electrophilicity index. *J. Am. Chem. Soc.* 121 (1999) 1922-1924.
- [26] R. Ahmadi, R. Soleymani, The influence of tyrozine on energetic property in graphene oxide: A DFT studies. *Orient. J. Chem.* 30 (2014) 57-62.
- [27] R. Soleymani, R.D. Dijvejin, A.F.G.A.Hesar, E. Sobhanie, Synthesis 4-(4/-methylphenyl)-2-mercaptothiazole structure with NMR, vibrational, Mass spectroscopy and DFT studies. *Oriental Journal of Chemistry.* 28 (2012) 1291-1304.
- [28] R. Soleymani, Y. Mohammad Salehi, T. Yousofzad, M. Karimi-Cheshmeh Ali, Synthesis, NMR, vibrational and Mass Spectroscopy with DFT/HF studies of 4-(4/-Bromophenyl)-2-mercaptothiazole structure. *Orient. J. Chem.* 28 (2012) 627-638.
- [29] J.J. McKinnon, D. Jayatilaka, M.A. Spackman, *ChemCommun.*37 (2007) 3814-3816.
- [30] J.J. Koenderink, *Solid Shape*, Cambridge MA, MIT Press.(1990).
- [31] M.J. Frisch, G.W. Trucks, H.B. Schlegel, G.E. Scuseria, M.A. Robb, J.R. Cheeseman, J.A. Montgomery, T. Vreven, K.N. Kudin, J.C. Burant, J.M. Millam, S.S. Iyengar, J. Tomasi, V. Barone, B. Mennucci, M. Cossi, G. Scalmani, N. Rega, G.A. Petersson, H. Nakatsuji, M. Hada, M. Ehara, K. Toyota, R. Fukuda, J. Hasegawa, M. Ishida, T. Nakajima, Y. Honda, O. Kitao, H. Nakai, M. Klene, X. Li, J.E. Knox, H.P. Hratchian, J.B. Cross, C. Adamo, J. Jaramillo, R. Gomperts, R.E. Stratmann, O. Yazyev, A.J. Austin, R. Cammi, C. Pomelli, J.W. Ochterski, P.Y. Ayala, K. Morokuma, G.A. Voth, P. Salvador, J.J. Dannenberg, V.G. Zakrzewski, S. Dapprich, A.D. Daniels, M.C. Strain, O. Farkas, D.K. Malick, A.D. Rabuck, K. Raghavachari, J.B. Foresman, J.V. Ortiz, Q. Cui, A.G. Baboul, S. Clifford, J. Cioslowski, B.B. Stefanov, G. Liu, A. Liashenko, P. Piskorz, I. Komaromi, R.L. Martin, D.J. Fox, T. Keith, M.A. Al-Laham, C.Y.

- Peng, A. Nanayakkara, M. Challacombe, P.M.W. Gill, B. Johnson, W. Chen, M.W. Wong, C. Gonzalez, J.A. Pople, Gaussian 03 Revision C.02, Gaussian Inc., Pittsburgh, PA, (2003).
- [32] M.H Jamroz, Vibrational Energy Distribution Analysis VEDA 4, Warsaw.(2004).
- [33] Computational Chemistry Comparison and Benchmark DataBase, Release 17b, September, NIST Standard Reference Database 10 (2015).
- [34] S.K.Wolff,D.J.Grimwood,J.J.McKinnon,D.Jayatilaka,and M. A. Spackman, CrystalExplorer, Version 1. 5, University of Western Australia, Perth, Australia, (2007).
- [35] C. F. Macrae, I. J. Bruno, J. A. Chisholm, P. R. Edgington, P. McCabe, E. Pidcock, L. Rodriguez-Monge, R. Taylor, J. van de Streek and P. A. Wood, Mercury CSD 2.0 – new features for the visualization and investigation of crystal structures. *J. Appl. Cryst.* 41 (2008) 466-470.
- [36] P. Flükinger, H. P. Lüthi, S. Portmann, and J. Weber, Molekel 4.3, Swiss Center for Scientific Computing, Manno.(2000).
- [37] D.M. Suresh, M. Amalanathan, S. Sebastian, D. Sajan, I. Hubert Joe, V. BenaJothy, Ivan Nemeč, Vibrational spectral investigation and natural bond orbital analysis of pharmaceutical compound 7-Amino-2,4-dimethylquinolinium formate – DFT approach. *Spectrochim. Acta Part A.* 115 (2013) 595-602.
- [38] M. NadeemArshad, A. Bibi, T. Mahmood, A. M. Asiri, and K. Ayub, Synthesis, crystal structures and spectroscopic properties of triazine-based hydrazone derivatives; A comparative experimental-theoretical study. *Molecules* 20 (2015) 5851-5874.
- [39] M.K. Rofouei, N. Sohrabi, M. Shamsipur, E. Fereyduni, S. Ayyappan, N. Sundaraganesan, X-ray crystallography characterization, vibrational spectroscopy, NMR spectra and quantum chemical DFT/HF study of N,N'-di(2-methoxyphenyl)formamidine. *Spectrochim. Acta Part A* 76 (2010) 182-190.

- [40] M.K. Rofouei, E. Fereyduni, N. Sohrabi, M. Shamsipur, J. Attar Gharamaleki, N. Sundaraganesan, Synthesis, X-ray crystallography characterization, vibrational spectroscopic, molecular electrostatic potential maps, thermodynamic properties studies of N,N'-di(p-thiazole)formamidine. *Spectrochim. Acta Part A* 78 (2011) 88-95.
- [41] A.A. Soayed, H.M. Refaat, L. Sinha, Syntheses, structural elucidation, thermal properties, theoretical quantum chemical studies (DFT) and biological studies of barbituric-hydrazone complexes. *J. Saudi Chem. Soc.* 19 (2015) 217-226.
- [42] M. Wainwright, Background and Theory Page of Nuclear Magnetic Resonance Facility, Analytical Centre - University of Southern Wales Sydney (2014).
- [43] N. Shah, A. Sattar, M. Benanti, S. Hollander, L. Cheuck, Magnetic resonance spectroscopy as an imaging tool for cancer: A review of the literature. *J. Am. Osteopathic Assoc.* 106 (2006) 23-27.
- [44] R. D. Dejvejen, G. Zarei, R. Soleymani, NMR, aromaticity and energetic property in $C_6H_4O_2M$ (M=C, S, O and N) dicarbaldehyde derivatives: A computational study. *Orient. J. Chem.* 28 (2012) 1229-1240.
- [45] R. Soleymani, M. Karimi-Cheshmeh Ali, N. Niakan, NMR Studies of BH₃-attaching in the zigzag and armchair BN nanotubes: A DFT study. *Orient. J. Chem.* 28 (2012)815-827.

Table Captions:

Table 1. Crystal data and structure refinement.

Table 2. Computed and experimental bond distances (Å), bond angles (°), torsion angles (°) for (CNPMPT) structure.

Table 3. Vibrational wavenumbers obtained for (CNPMPT) structure at B3LYP, B3PW91 and PBEPBE levels of theory with 6-311G (d,p) basis set [harmonic frequency (cm^{-1}), IRint (Kmol^{-1})].

Table 4. Theoretical and experimental ^1H and ^{13}C isotropic chemical shifts (with respect to TMS, all values in ppm) for (CNPMPT) structure.

Table 5. Theoretically computed energies (kcal.mol^{-1}), zero-point vibrational energies (kcal.mol^{-1}), rotational constants (GHz), heat capacities ($\text{cal.mol}^{-1}.\text{K}^{-1}$), entropies ($\text{cal.mol}^{-1}.\text{K}^{-1}$), dipole moment (Debye), molecular orbitals energies (ϵ_{HOMO} and ϵ_{LUMO} , eV), electronic chemical potential, μ (eV), chemical hardness, η (eV), electrophilicity, ω (eV) and maximum amount of electronic charge transfer for (CNPMPT) structure.

Scheme Captions:

Scheme 1. Synthetic route for the new compound (CNPMPT).

Figure Captions:

Fig. 1. Serial number of atom and optimized structure of (CNPMPT) structure performed by B3LYP/6-311G (d, p) method (a), different conformations of the title compound (b).

Fig. 2. A view of the hydrogenbonds are shown as dashed lines (a) and crystal packing down the α -axis for the title compound (b).

Fig. 3. FT-IR spectrum obtained by experimental (a) in terms of percentage transmission and DFT method (b) in terms of intensity for (CNPMPT) structure.

Fig. 4. B3LYP/6-311G (d, p) calculated 3D molecular electrostatic potential of CNPMPT (isosurfacevalue 0.01 a.u.).

Fig. 5. Show 3D and 2D images of fingerprint plots and corresponding Hirshfield surface coverage for CNPMPT structure.

Supplementary Data Captions:

S1. Correlation between bond length obtained by experimental (X-Ray diffraction) and theoretical value (DFT method) for the title compound.

S2. Correlation between DFT and experimental frequencies for the title compound.

S3. Show ^{13}C (a) and ^1H (b) NMR spectrum obtained by experimental methods for the title compound.

S4. Correlation between theoretical and experimental methods for NMR property in (CNPMPT) structure.

S5. Show E (a) and Z (b) conformation of (CNPMPT) structure.

S6. Show density of spectrum (Dos) and HOMO-LUMO highlight obtained by B3LYP level of theory for CNPMPT structure.

Table 1.

| | |
|---|--|
| Empirical formula | C ₁₃ H ₁₁ ClN ₄ O ₃ |
| Formula weight | 306.7 |
| Temperature (K) | 298 (2) |
| Wavelength (Å) | 0.71073 |
| Crystal system, space group | Orthorhombic, <i>Pbca</i> |
| Unit cell dimensions | |
| <i>a</i> (Å), α (°) | 7.0723 (9), 82.448 (9) |
| <i>b</i> (Å), β (°) | 7.5333 (9), 79.931 (9) |
| <i>c</i> (Å), γ (°) | 13.7138 (15), 75.049 (9) |
| Volume (Å ³) | 692.17 (15) |
| Z, Calculated density (Mg/m ³) | 2, 1.472 |
| Absorption coefficient (mm ⁻¹) | 0.292 |
| <i>F</i> (000) | 316 |
| Crystal size (mm) | 0.4×0.20×0.15 |
| Theta range for data collection (deg) | 2.81 to 29.20 |
| Max/min. indices <i>h, k, l</i> | -9/8, -10/9, -18/18 |
| Reflections collected | 7537 |
| Independent reflections [<i>R</i> (int)] | 3704 [0.0899] |
| Completeness to theta = 27.00 (%) | 98.7 |
| Refinement method | Full-matrix least-squares on <i>F</i> ² |
| Data / restraints / parameters | 3704/0/195 |
| Goodness-of-fit on <i>F</i> ² | 0.993 |
| Final <i>R</i> indices [<i>I</i> > 2σ(<i>I</i>)] | <i>R</i> ₁ = 0.0703, ω <i>R</i> ₂ = 0.1722 |
| <i>R</i> indices (all data) | <i>R</i> ₁ = 0.1420, ω <i>R</i> ₂ = 0.2120 |
| Largest diff. peak and hole (e.Å ⁻³) | 0.470 and -0.436 |

Table 2.

| Parameters | X-ray | B3LYP | B3PW91 | PBEPBE |
|------------------------|-----------|-------|--------|--------|
| Bond length (Å) | | | | |
| Cl32-C13 | 1.722 (3) | 1.744 | 1.730 | 1.741 |
| O23-C4 | 1.368 (4) | 1.357 | 1.351 | 1.363 |
| O23-C24 | 1.417 (4) | 1.422 | 1.415 | 1.429 |
| O30-N28 | 1.202 (4) | 1.224 | 1.218 | 1.234 |
| O29-N28 | 1.191 (4) | 1.219 | 1.214 | 1.230 |
| N20-N21 | 1.328 (3) | 1.324 | 1.318 | 1.328 |
| N20-C3 | 1.395 (4) | 1.408 | 1.402 | 1.399 |
| N21-N22 | 1.261 (3) | 1.262 | 1.260 | 1.282 |
| N22-C16 | 1.420 (3) | 1.409 | 1.404 | 1.406 |
| N20-C14 | 1.472 (4) | 1.480 | 1.474 | 1.486 |
| C4-C5 | 1.382 (4) | 1.396 | 1.394 | 1.404 |
| C4-C3 | 1.396 (4) | 1.415 | 1.412 | 1.425 |
| C5-C6 | 1.379 (6) | 1.395 | 1.392 | 1.399 |
| C6-C1 | 1.382 (5) | 1.389 | 1.387 | 1.396 |
| C1-C2 | 1.374 (5) | 1.392 | 1.390 | 1.394 |
| C2-C3 | 1.387(5) | 1.395 | 1.393 | 1.407 |
| C16-C15 | 1.381 (4) | 1.394 | 1.392 | 1.402 |
| C16-C11 | 1.395 (4) | 1.404 | 1.402 | 1.413 |
| C15-C14 | 1.386 (4) | 1.390 | 1.387 | 1.395 |
| C14-C13 | 1.386 (4) | 1.398 | 1.396 | 1.406 |
| C13-C12 | 1.385 (4) | 1.397 | 1.396 | 1.405 |
| C12-C11 | 1.372 (4) | 1.385 | 1.382 | 1.390 |
| Bond Angles (°) | | | | |
| C4-O23-C24 | 118.5 (3) | 118.6 | 118.3 | 117.7 |
| N21-N20-C3 | 121.2 (3) | 123.8 | 123.9 | 126.9 |
| N22-N21-N20 | 112.4 (2) | 112.5 | 112.3 | 111.0 |
| N21-N22-C16 | 112.4 (2) | 113.9 | 113.7 | 113.4 |
| O29-N28-O30 | 122.4 (3) | 125.4 | 125.6 | 125.7 |
| O29-N28-C14 | 119.6 (3) | 117.9 | 117.8 | 117.7 |
| O30-N28-C14 | 117.8 (3) | 116.7 | 116.6 | 116.6 |
| O23-C4-C5 | 125.9 (3) | 124.2 | 124.2 | 123.9 |
| O23-C4-C3 | 114.3 (2) | 117.0 | 117.1 | 117.5 |
| C5-C4-C3 | 119.8 (3) | 118.7 | 118.7 | 118.6 |
| C6-C5-C4 | 119.9 (3) | 120.9 | 121.0 | 121.5 |
| C5-C6-C1 | 120.2 (3) | 120.3 | 120.3 | 120.0 |
| C2-C1-C6 | 120.4 (3) | 119.3 | 119.2 | 119.3 |
| C1-C2-C3 | 119.8 (3) | 121.2 | 121.3 | 121.7 |
| C2-C3-N20 | 123.1 (3) | 118.0 | 117.9 | 116.2 |
| C2-C3-C4 | 119.8 (3) | 119.5 | 119.5 | 119.0 |
| N20-C3-C4 | 117.1 (3) | 122.4 | 122.5 | 124.8 |
| C15-C16-C11 | 118.9 (2) | 118.7 | 118.6 | 118.5 |
| C15-C16-N22 | 116.0 (3) | 115.9 | 115.9 | 116.0 |
| C11-C16-N22 | 125.1 (2) | 125.4 | 125.4 | 125.6 |
| C16-C15-C14 | 120.4 (3) | 120.7 | 120.7 | 120.9 |
| C13-C14-C15 | 120.9 (3) | 120.8 | 120.9 | 120.7 |
| C13-C14-N28 | 122.7 (2) | 122.9 | 122.8 | 123.0 |
| C15-C14-N28 | 116.4 (3) | 116.2 | 116.2 | 116.3 |
| C12-C13-C14 | 118.2 (2) | 118.3 | 118.2 | 118.3 |
| C12-C13-Cl32 | 117.8 (2) | 118.0 | 118.1 | 118.0 |

| | | | | |
|---------------------------|------------|--------|--------|--------|
| C14-C13-C132 | 124.0 (2) | 123.7 | 123.7 | 123.7 |
| C11-C12-C13 | 121.5 (3) | 121.2 | 121.2 | 121.2 |
| C12-C11-C16 | 120.1 (3) | 120.3 | 120.4 | 120.4 |
| Dihedral Angles(°) | | | | |
| C3-N20-N21-N22 | 177.3 (3) | 176.0 | 176.5 | 179.6 |
| N20-N21-N22-C16 | -179.5 (2) | -179.1 | -179.4 | -179.8 |
| C24-O23-C4-C5 | -6.7 (5) | -3.0 | -3.0 | -1.0 |
| C24-O23-C4-C3 | 173.5 (3) | 175.9 | 175.8 | 178.7 |
| O23-C4-C5-C6 | -179.5 (3) | -177.4 | -177.3 | -179.5 |
| C3-C4-C5-C6 | 0.3 (5) | 1.5 | 1.5 | 0.2 |
| C4-C5-C6-C1 | -0.1 (6) | -0.2 | -0.2 | -0.0 |
| C5-C6-C1-C2 | 0.1 (6) | 1.0 | 1.0 | 0.2 |
| C6-C1-C2-C3 | -0.3 (5) | -0.8 | -0.8 | -0.1 |
| C1-C2-C3-N20 | -179.6 (3) | -177.0 | -177.0 | -179.5 |
| C1-C2-C3-C4 | 0.5 (5) | 0.5 | 0.6 | 0.1 |
| N21-N20-C3-C2 | -3.3 (5) | -40.6 | -39.8 | -5.3 |
| N21-N20-C3-C4 | 176.6 (3) | 143.0 | 143.9 | 175.4 |
| O23-C4-C3-C2 | 179.4 (3) | 177.3 | 177.2 | 179.5 |
| C5-C4-C3-C2 | -0.5 (5) | -1.6 | -1.7 | -0.3 |
| O23-C4-C3-N20 | -0.5 (4) | -0.5 | -0.9 | -0.2 |
| C5-C4-C3-N20 | 179.6 (3) | 177.9 | 178.0 | 179.6 |
| N21-N22-C16-C15 | -175.6 (3) | -176.0 | -177.1 | -179.5 |
| N21-N22-C16-C11 | 6.4 (4) | 4.8 | 3.6 | 0.9 |
| C11-C16-C15-C14 | -1.9 (5) | -1.4 | -1.4 | -1.4 |
| N22-C16-C15-C14 | 180.0 (3) | 179.4 | 179.2 | 179.0 |
| C16-C15-C14-C13 | 1.5 (5) | 1.6 | 1.6 | 1.6 |
| C16-C15-C14-N28 | -178.9 (3) | -178.0 | -178.0 | 178.1 |
| O29-N28-C14-C13 | -22.3 (5) | -37.4 | -37.9 | -35.3 |
| O30-N28-C14-C13 | 163.1 (3) | 144.2 | 143.7 | 146.1 |
| O29-N28-C14-C15 | 158.1 (4) | 142.2 | 141.7 | 144.3 |
| O30-N28-C14-C15 | -16.5 (4) | -36.1 | -36.6 | -34.3 |
| C15-C14-C13-C12 | -0.2 (5) | -0.4 | -0.5 | -0.3 |
| N28-C14-C13-C12 | -179.8 (3) | -179.2 | -179.1 | -179.3 |
| C15-C14-C13-C132 | 178.1 (2) | 176.4 | 176.4 | 176.6 |
| N28-C14-C13-C132 | -1.5 (4) | -4.0 | -4.0 | -3.8 |
| C14-C13-C12-C11 | -0.6 (5) | -0.9 | -0.9 | -1.1 |
| C132-C13-C12-C11 | -179.1 (3) | -177.9 | -177.9 | -178.2 |
| C13-C12-C11-C16 | 0.2 (5) | 1.0 | 1.1 | 1.2 |
| C15-C16-C11-C12 | 1.1 (5) | 0.2 | 0.1 | 0.0 |
| N22-C16-C11-C12 | 179.0 (3) | 179.3 | 179.4 | 179.5 |

Table 3.

| Mod nos. | Experimental (cm ⁻¹) FT-IR | Theoretical wavenumber (cm ⁻¹) | | | | | | PED(%) ^c |
|-------------|--|--|--------------------------------|--------|--------------------------------|--------|--------------------------------|---|
| | | B3LYP | | B3PW91 | | PBEPBE | | |
| | | Scaled | IR _{int} ^b | Scaled | IR _{int} ^b | Scaled | IR _{int} ^b | |
| 1 | 3305s | 3351 | 14.44 | 3353 | 16.44 | 3290 | 4.63 | 100 v NH |
| 2 | | 3117 | 4.07 | 3111 | 4.51 | 3123 | 4.10 | 45 v CH + 51 v CH |
| 3 | | 3109 | 0.90 | 3105 | 0.99 | 3117 | 8.65 | 49 v CH + 21 v CH + 30 v CH |
| 4 | | 3104 | 7.77 | 3100 | 6.73 | 3116 | 1.69 | 27 v CH + 13 v CH + 52 v CH |
| 5 | 3090vw | 3091 | 1.40 | 3090 | 14.35 | 3107 | 15.36 | 75 v CH + 19 v CH |
| 6 | | 3090 | 18.45 | 3087 | 1.27 | 3100 | 2.01 | 25 v CH + 38 v CH + 36 v CH |
| 7 | | 3073 | 5.94 | 3072 | 4.23 | 3089 | 1.84 | 44 v CH + 28 v CH + 27 v CH |
| 8 | 3013vw | 3062 | 5.72 | 3060 | 5.48 | 3068 | 7.28 | 26 v CH + 59 v CH + 11 v CH |
| 9 | 2977vw | 3035 | 14.87 | 3037 | 13.11 | 3051 | 11.10 | 79 v CH + 21 v CH |
| 10 | 2944w | 2965 | 35.45 | 2967 | 32.23 | 2976 | 32.39 | 99 v CH |
| 11 | 2840vw | 2907 | 54.10 | 2902 | 53.18 | 2912 | 61.22 | 21 v CH + 79 v CH |
| 12 | 1599s | 1591 | 71.49 | 1612 | 201.65 | 1583 | 33.46 | 23 v ON + 40 v CC |
| 13 | | 1587 | 29.20 | 1596 | 32.13 | 1581 | 16.10 | 27 v CC + 14 v CC + 11 v CC + 13 δ HCC |
| 14 | | 1575 | 10.12 | 1587 | 59.41 | 1570 | 10.05 | 14 v CC + 30 v CC + 10 v CC + 11 δ CCC + 13 δ CCC |
| 15 | 1569w | 1567 | 154.55 | 1582 | 5.83 | 1549 | 137.43 | 55 v ON + 23 v CC |
| 16 | 1523s | 1540 | 22.63 | 1550 | 4.86 | 1528 | 50.94 | 12 v ON + 17 v CC + 28 v CC + 12 δ CCC + 16 δ CCC |
| 17 | 1514s | 1500 | 482.56 | 1508 | 612.61 | 1500 | 347.69 | 13 v NN + 13 v NC + 40 δ HNN |
| 18 | 1476vw | 1489 | 39.26 | 1488 | 41.74 | 1480 | 48.76 | 10 δ HNN + 38 δ HCC + 13 δ CCC |
| 19 | 1463s | 1459 | 139.48 | 1466 | 179.77 | 1440 | 39.63 | 25 v NN + 31 δ HCH |
| 20 | | 1453 | 21.21 | 1449 | 228.69 | 1437 | 186.58 | 20 v NN + 35 δ HCH + 10 Γ HCOC |
| 21 | | 1449 | 264.36 | 1445 | 25.70 | 1425 | 9.02 | 44 δ HCC + 12 δ CCC |
| 22 | 1442vw | 1444 | 8.83 | 1434 | 8.96 | 1424 | 128.95 | 68 δ HCH + 23 Γ HCOC |
| 23 | 1422w | 1434 | 13.96 | 1425 | 5.32 | 1411 | 89.37 | 68 δ HCH |
| 24 | | 1410 | 20.97 | 1404 | 12.45 | 1394 | 26.93 | 13 v CC + 32 δ HCC + 10 δ HCH |
| 25 | 1386m | 1376 | 55.10 | 1380 | 31.62 | 1369 | 207.61 | 42 v CC + 17 δ HCC |
| 26 | 1342s | 1339 | 280.53 | 1364 | 296.85 | 1351 | 18.96 | 78 v ON + 12 δ ONO |

| | | | | | | | | |
|----|--------|------|--------|------|--------|------|--------|---|
| 27 | 1314vw | 1302 | 13.67 | 1321 | 18.02 | 1325 | 51.50 | 24 ν CC + 13 ν CC + 10 ν CC + 12 ν CC |
| 28 | | 1292 | 88.25 | 1311 | 76.13 | 1307 | 295.27 | 52 ν CC |
| 29 | | 1269 | 43.60 | 1269 | 323.82 | 1262 | 262.00 | 11 ν OC + 39 δ HCC |
| 30 | 1256m | 1255 | 426.58 | 1259 | 189.95 | 1258 | 139.49 | 12 ν NN + 14 ν OC + 10 δ HNN |
| 31 | | 1243 | 6.77 | 1243 | 58.63 | 1237 | 60.59 | 12 ν NC + 44 δ HCC |
| 32 | 1218w | 1220 | 281.02 | 1227 | 254.05 | 1223 | 148.67 | 13 ν NN + 17 ν OC + 10 ν NC |
| 33 | 1197vw | 1191 | 85.64 | 1194 | 18.10 | 1187 | 4.52 | 15 ν CC + 27 ν NC + 14 δ HCC |
| 34 | | 1184 | 135.30 | 1192 | 87.74 | 1183 | 88.16 | 10 ν CC + 32 ν NN + 13 ν NC |
| 35 | 1157vw | 1165 | 29.04 | 1160 | 14.48 | 1154 | 11.95 | 21 δ HCH + 54 Γ HCOC |
| 36 | 1145vw | 1148 | 6.17 | 1140 | 4.90 | 1141 | 0.16 | 72 δ HCC |
| 37 | | 1131 | 1.13 | 1126 | 0.86 | 1115 | 15.15 | 24 δ HCH + 62 Γ HCOC + 12 Γ HCOC |
| 38 | | 1127 | 6.39 | 1120 | 8.40 | 1115 | 0.33 | 60 δ HCC |
| 39 | 1109m | 1110 | 51.83 | 1108 | 45.81 | 1110 | 50.89 | 13 ν CC + 14 ν CC + 39 δ HCC |
| 40 | | 1093 | 34.87 | 1097 | 35.05 | 1084 | 35.29 | 18 ν CC + 11 ν CIC + 31 δ HCC |
| 41 | 1042m | 1040 | 15.62 | 1042 | 24.60 | 1043 | 7.21 | 17 ν CC + 19 ν CC + 10 ν OC + 23 δ HCC |
| 42 | 1027m | 1019 | 42.07 | 1027 | 26.34 | 1011 | 41.37 | 10 ν CIC + 47 δ CCC |
| 43 | | 1017 | 43.27 | 1020 | 41.09 | 1009 | 51.29 | 10 ν CC + 57 ν OC + 14 δ CCC |
| 44 | | 969 | 0.02 | 962 | 0.02 | 946 | 0.08 | 31 Γ HCCC + 51 Γ HCCC |
| 45 | | 949 | 0.72 | 950 | 0.93 | 945 | 2.17 | 10 δ CCC + 15 δ CCC + 12 δ NNN |
| 46 | 919vw | 940 | 0.27 | 938 | 0.24 | 915 | 0.01 | 12 Γ HCCC + 68 Γ HCCC + 16 Γ CCCN |
| 47 | | 902 | 18.86 | 898 | 5.72 | 880 | 18.47 | 23 Γ HCCC + 30 Γ HCCC + 16 Γ CCCC |
| 48 | 892w | 901 | 2.69 | 894 | 17.24 | 873 | 14.27 | 77 Γ HCCC |
| 49 | | 877 | 14.60 | 878 | 16.28 | 871 | 4.46 | 15 δ ONO + 23 δ CCC |
| 50 | 831w | 826 | 19.56 | 822 | 0.61 | 809 | 17.65 | 71 Γ HCCC + 10 Γ CCCC |
| 51 | 816vw | 826 | 0.62 | 821 | 20.87 | 805 | 23.68 | 75 Γ HCCC |
| 52 | 783vw | 810 | 21.61 | 812 | 21.37 | 799 | 0.18 | 29 δ ONO + 18 δ CCC |
| 53 | 747s | 759 | 10.53 | 762 | 8.03 | 756 | 6.17 | 10 ν CC + 13 ν OC + 10 δ CCC |
| 54 | | 751 | 8.78 | 756 | 9.64 | 739 | 4.17 | 57 λ OCON + 14 λ NCCC |
| 55 | 724vw | 733 | 79.55 | 731 | 84.91 | 720 | 119.06 | 88 Γ HCCC |
| 56 | | 719 | 12.62 | 718 | 13.78 | 707 | 2.38 | 23 Γ CCCN + 18 λ OCCC |
| 57 | | 700 | 11.07 | 700 | 10.02 | 700 | 21.24 | 13 δ CCC + 13 δ CCC |
| 58 | 685vs | 691 | 10.73 | 690 | 12.41 | 681 | 15.78 | 22 Γ HCCC + 24 Γ CCCC |

| | | | | | | | | |
|----|-------|-----|-------|-----|-------|-----|-------|--|
| 59 | 673w | 664 | 23.08 | 662 | 22.64 | 679 | 14.94 | 24 δ CCC + 11 δ CCC |
| 60 | 649w | 635 | 13.08 | 634 | 36.52 | 659 | 24.17 | 12 δ NNC + 12 δ CCC + 10 δ CNN + 15 Γ HNNN |
| 61 | 633m | 622 | 26.49 | 623 | 47.18 | 630 | 14.20 | 12 δ ONC |
| 62 | | 612 | 91.17 | 617 | 41.49 | 615 | 5.36 | 69 Γ HNNN |
| 63 | 577vw | 568 | 12.94 | 567 | 12.01 | 564 | 4.35 | 20 δ CCC |
| 64 | 553vw | 546 | 0.94 | 545 | 1.01 | 541 | 3.94 | 11 Γ HCCC + 43 Γ CCCN + 16 λ OCCC |
| 65 | | 543 | 2.10 | 542 | 1.51 | 540 | 0.49 | 10 δ CCC + 10 δ COC |
| 66 | | 508 | 6.57 | 506 | 7.35 | 504 | 5.88 | 10 δ CCN |
| 67 | 483m | 482 | 12.82 | 482 | 12.73 | 468 | 17.88 | 12 δ ONC + 10 δ CCC |
| 68 | | 456 | 7.964 | 454 | 8.88 | 455 | 2.92 | 14 Γ CCCN + 22 Γ CCCN + 14 λ OCCC |
| 69 | | 428 | 13.64 | 428 | 12.44 | 426 | 13.98 | 11 ν NC + 12 δ CICC + 11 Γ CCCC |
| 70 | | 409 | 2.13 | 407 | 1.73 | 407 | 4.32 | 33 Γ CCCC |
| 71 | | 363 | 0.48 | 361 | 0.32 | 364 | 0.59 | 14 δ COC |
| 72 | | 358 | 2.34 | 357 | 2.88 | 350 | 3.41 | 28 Γ CCCC + 22 Γ NNNC + 29 λ CCCCC |
| 73 | | 349 | 3.86 | 350 | 3.45 | 346 | 3.65 | 15 ν NC + 11 ν CIC + 13 δ CCC + 16 δ ONC |
| 74 | | 306 | 4.51 | 306 | 4.03 | 301 | 0.11 | 10 δ COC + 17 Γ HCOC + 13 Γ CCCN |
| 75 | | 291 | 1.77 | 291 | 1.95 | 293 | 3.84 | 11 δ COC + 15 δ CICC + 10 Γ CCCN |
| 76 | | 252 | 0.32 | 253 | 0.27 | 248 | 0.17 | 36 Γ HCOC + 12 Γ CCCN |
| 77 | | 232 | 1.38 | 232 | 1.30 | 235 | 0.39 | 31 δ OCC + 19 δ COC |
| 78 | | 221 | 0.80 | 222 | 0.80 | 215 | 0.52 | 17 δ OCC + 15 δ COC |
| 79 | | 212 | 2.08 | 212 | 2.18 | 212 | 1.33 | 24 Γ NNNC + 13 λ CCCCC |
| 80 | | 189 | 4.97 | 189 | 5.07 | 178 | 0.69 | 17 δ NCC + 17 δ CICC |
| 81 | | 163 | 5.65 | 163 | 4.67 | 164 | 0.24 | 12 δ NCC + 14 Γ NNCC + 16 Γ CNNN + 10 λ NCCC |
| 82 | | 158 | 1.43 | 158 | 2.36 | 148 | 3.17 | 26 Γ CCCN + 11 Γ CCCN |
| 83 | | 117 | 2.43 | 117 | 2.13 | 120 | 2.62 | 11 Γ CCCN + 13 Γ CCCC + 15 Γ CCCC + 20 λ NCCC |
| 84 | | 108 | 1.72 | 108 | 1.86 | 115 | 0.33 | 13 δ CCN + 20 δ NCC |
| 85 | | 88 | 4.59 | 89 | 4.66 | 97 | 6.34 | 78 Γ COCC |
| 86 | | 73 | 0.98 | 73 | 0.81 | 74 | 0.06 | 34 Γ CCCC + 15 Γ CNNN + 10 λ CCCCC |
| 87 | | 51 | 0.34 | 51 | 0.36 | 50 | 0.30 | 83 Γ ONCC |
| 88 | | 38 | 0.18 | 39 | 0.16 | 39 | 0.20 | 23 δ NNC + 18 δ NNN + 24 δ CNN + 12 δ NCC |
| 89 | | 22 | 0.05 | 23 | 0.09 | 22 | 0.27 | 20 Γ NNCC + 40 Γ CCNN + 16 Γ CNNN |
| 90 | | 14 | 0.28 | 14 | 0.26 | 6 | 0.01 | 47 Γ NNCC + 22 Γ CCNN + 15 Γ CNNN |

^a w-weak; vw-very weak; s-strong; vs-very strong; m-medium; br-broad, sh-shoulder.

^b IR_{int}-IR intensity.

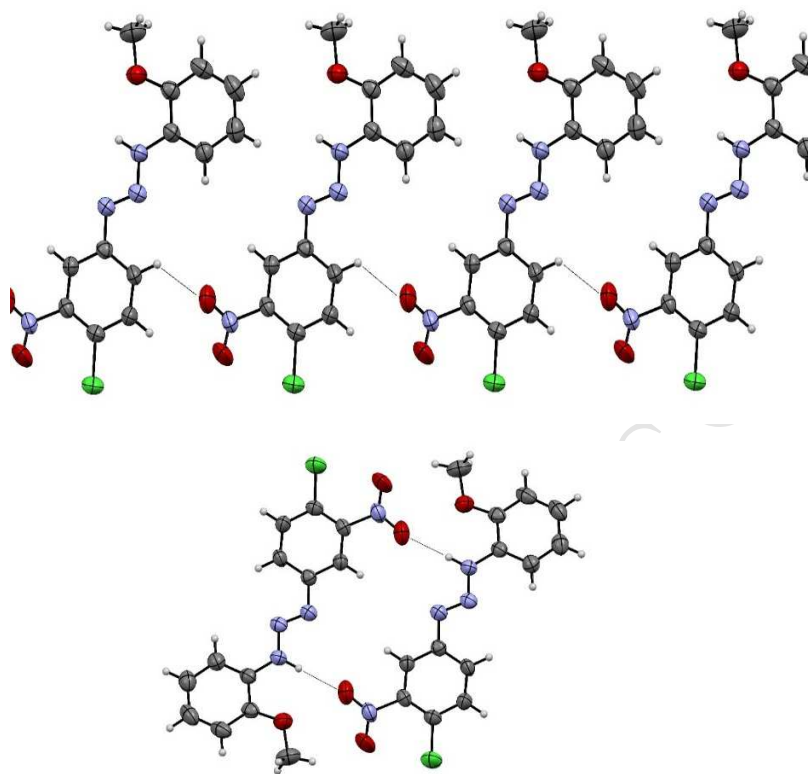
^c Potential energy distribution (PED) calculated B3LYP/6-311G (d, p). ν stretching, δ : bending, Γ : torsion, λ : out, PED less than 10% are not shown.

Table 4.

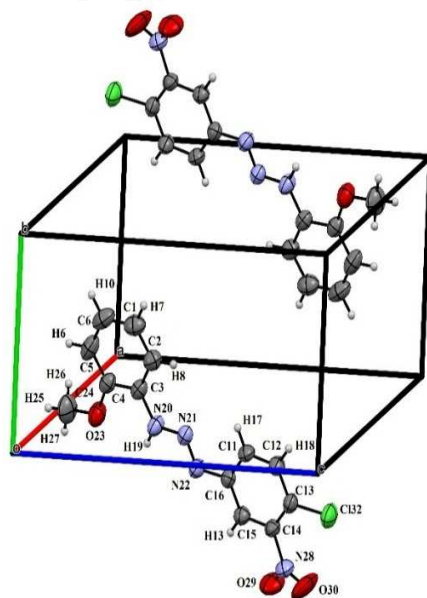
| | Label and symbol of atoms | Methods | | | Exp |
|----------------|------------------------------------|----------|----------|----------|---------|
| | | B3LYP | B3PW91 | PBEPBE | |
| Chemical Shift | C1 | 125.6611 | 124.0284 | 123.0390 | 125.704 |
| | C2 | 125.8774 | 124.2143 | 119.8860 | 125.829 |
| | C3 | 135.1938 | 132.2196 | 130.9738 | 134.198 |
| | C4 | 159.9869 | 156.6878 | 153.8458 | 159.909 |
| | C5 | 115.1109 | 113.6936 | 112.7329 | 113.140 |
| | C6 | 131.6540 | 130.0879 | 126.1705 | 131.088 |
| | C11 | 124.2204 | 122.6825 | 121.4266 | 124.522 |
| | C12 | 137.3123 | 135.7157 | 134.9075 | 137.483 |
| | C13 | 139.0023 | 135.3896 | 135.0595 | 138.086 |
| | C14 | 157.6784 | 154.3473 | 153.9157 | 157.266 |
| | C15 | 131.5964 | 129.9608 | 128.6155 | 130.807 |
| | C16 | 155.4771 | 152.5113 | 151.7045 | 155.950 |
| | C24 | 56.405 | 54.9586 | 57.2225 | 55.875 |
| | H7 | 7.0919 | 7.0646 | 7.0029 | 7.5157 |
| | H8 | 7.0811 | 7.0449 | 6.8168 | 7.5078 |
| | H9 | 6.8193 | 6.8102 | 6.812 | 7.4862 |
| | H10 | 7.2821 | 7.2536 | 7.0699 | 7.5396 |
| | H17 | 8.0199 | 8.008 | 7.9106 | 7.5659 |
| | H18 | 7.3498 | 7.3193 | 7.2529 | 7.5618 |
| | H19 | 8.9706 | 8.8945 | 9.2136 | 12.9728 |
| | H25 | 3.5573 | 3.4347 | 3.7699 | 3.8342 |
| | H26 | 3.8048 | 3.6805 | 3.6993 | 3.8342 |
| | H27 | 4.1371 | 4.0262 | 4.2198 | 3.8342 |
| | H31 | 8.1241 | 8.0855 | 7.9482 | 7.6686 |

Table 5.

| Parameters | B3LYP | P3PW91 | PBEPBE |
|------------------------------|--------------|--------------|--------------|
| Total energy | -882733.1034 | -882463.6636 | -881938.2729 |
| ZPVE | 145.47280 | 146.19423 | 141.38458 |
| Rotational constant | 0.73583 | 0.74212 | 0.74756 |
| | 0.10205 | 0.10258 | 0.10170 |
| | 0.09245 | 0.09302 | 0.09004 |
| Entropy | | | |
| Total | 146.169 | 145.804 | 149.562 |
| Translational | 43.052 | 43.052 | 43.052 |
| Rotational | 35.092 | 35.072 | 35.106 |
| Vibrational | 68.025 | 67.679 | 71.404 |
| Heat capacity | 69.157 | 68.918 | 71.026 |
| Dipole moment(D) | 8.73730 | 8.69640 | 8.57430 |
| HOMO | -0.22231 | -0.22399 | -0.19138 |
| LUMO | -0.09141 | -0.09168 | -0.11687 |
| Chemical potential(μ) | -0.15686 | -0.15783 | -0.15412 |
| Chemical hardness(η) | 0.13090 | 0.13231 | 0.07451 |
| Electrophilicity(ω) | 0.09398 | 0.09414 | 0.15940 |
| ΔN_{\max} | 1.19831 | 1.19291 | 2.06851 |

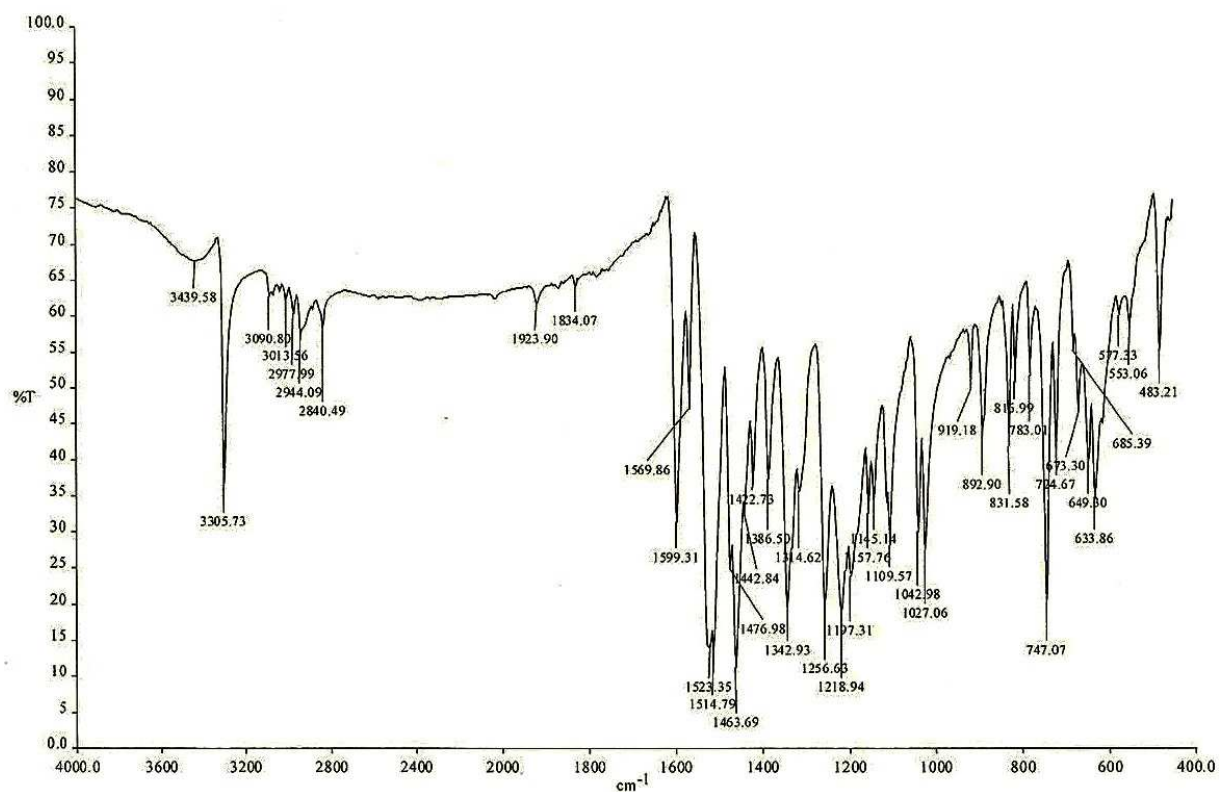


(a)

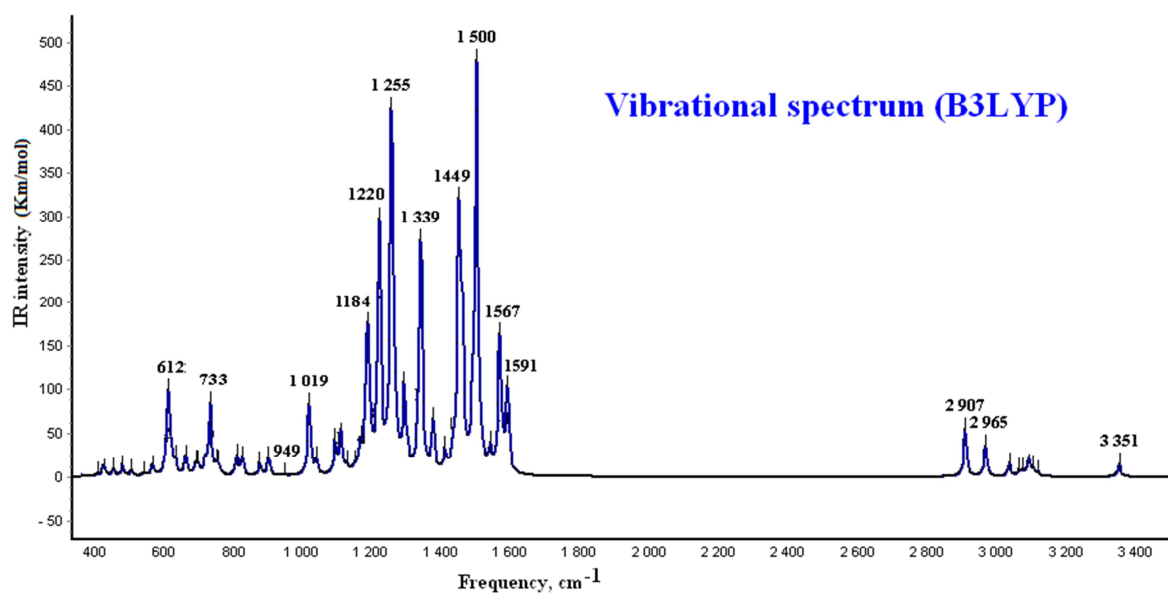


(b)

Fig. 2.

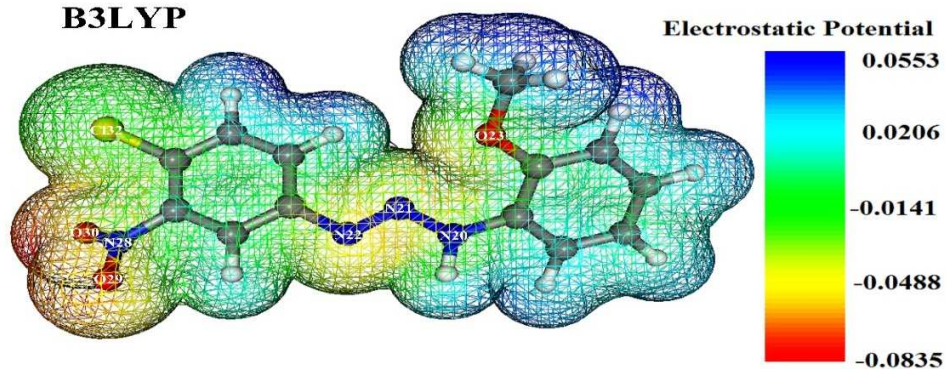


(a)

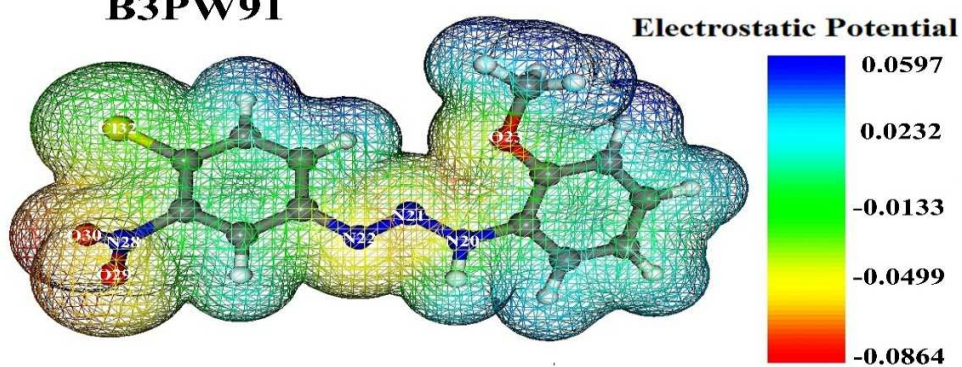


(b)

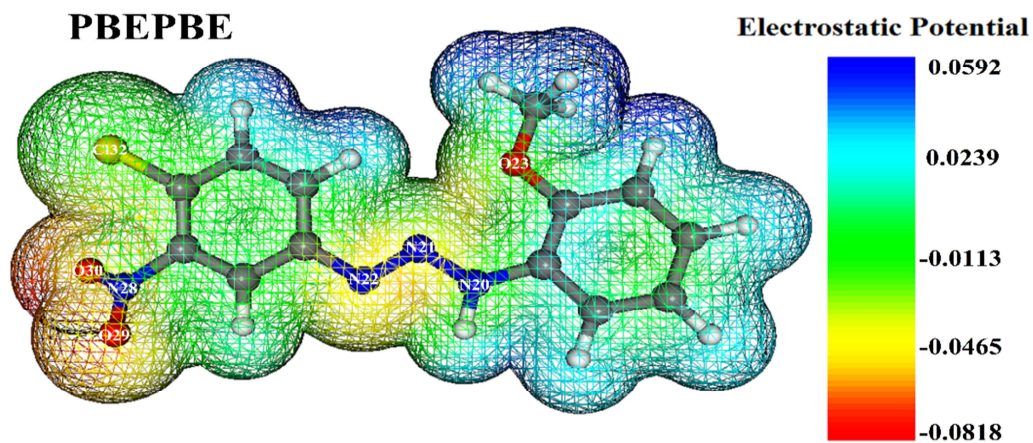
Fig 3.

B3LYP

(a)

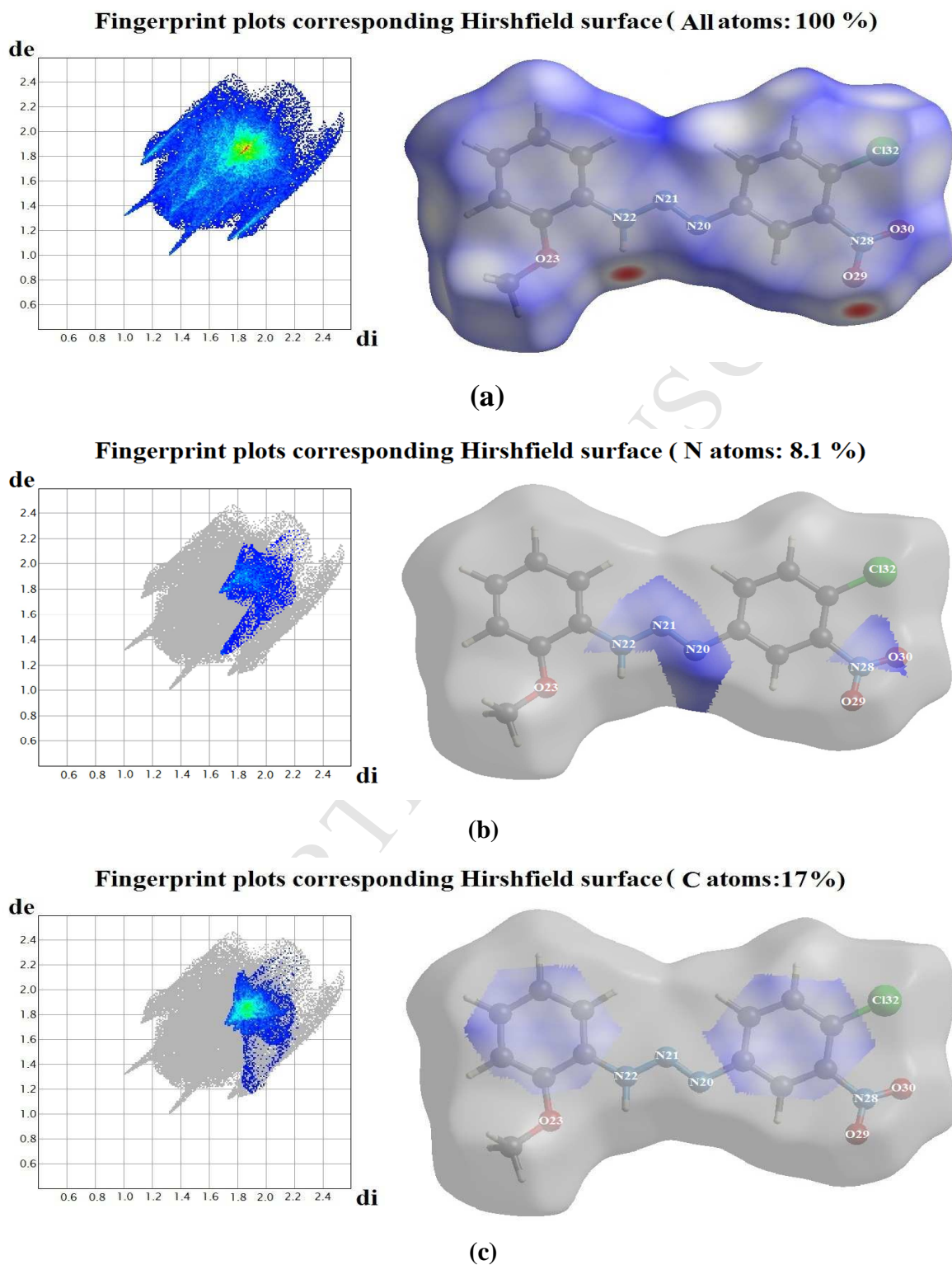
B3PW91

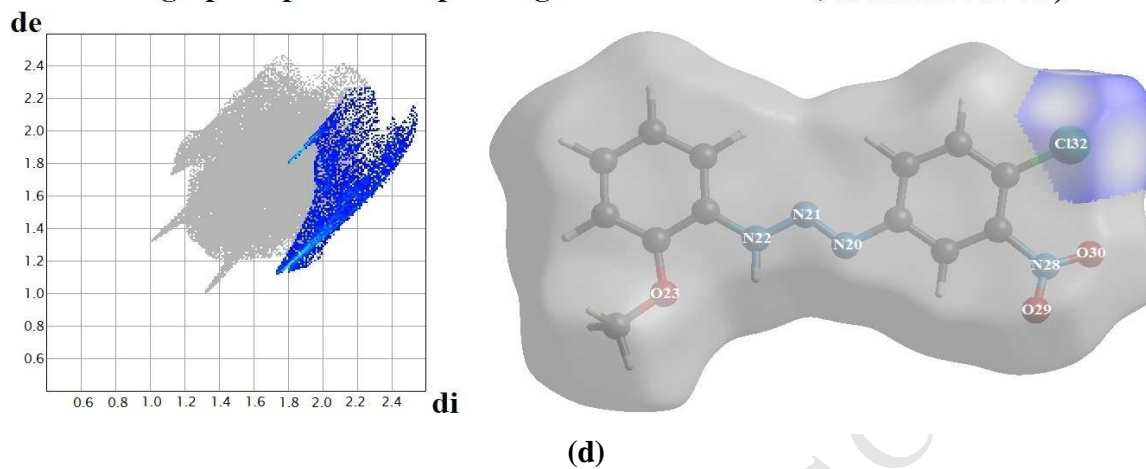
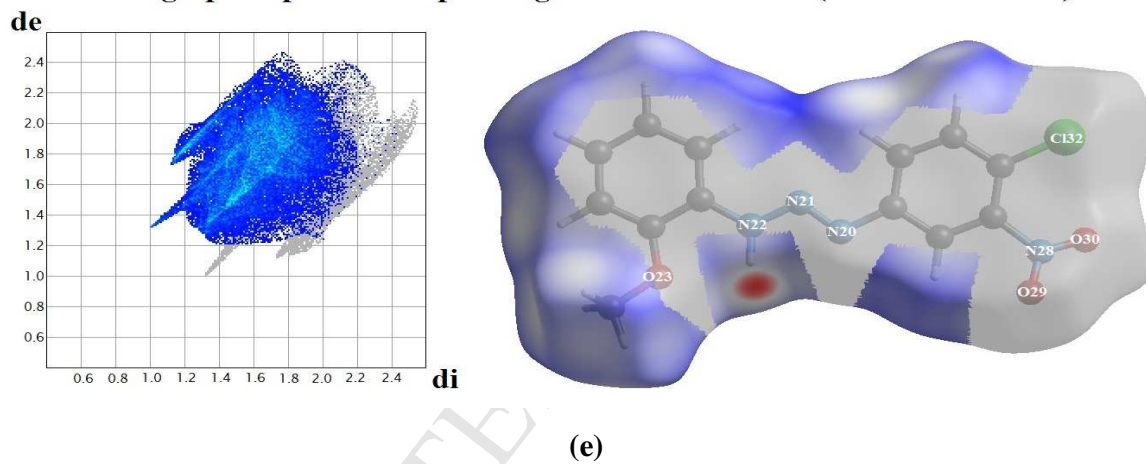
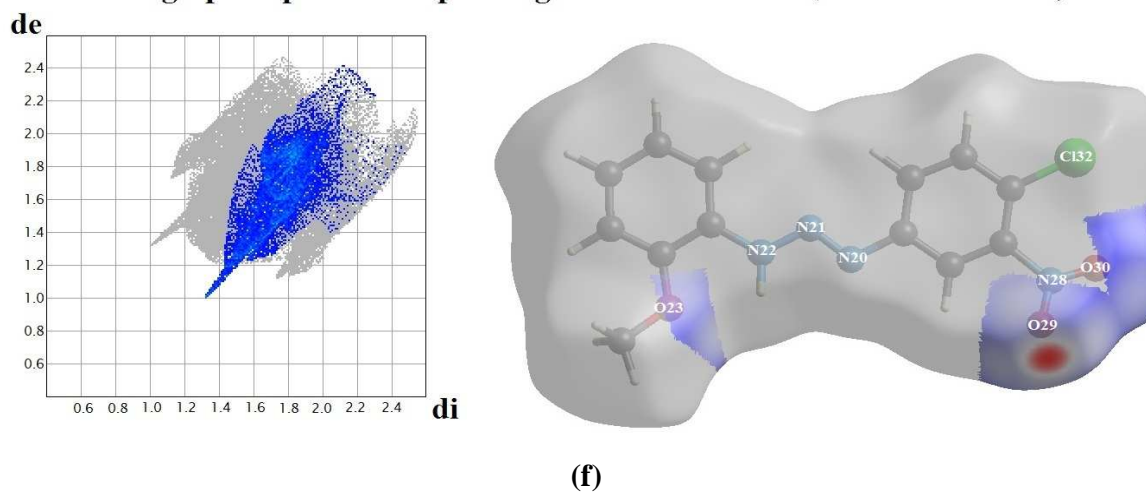
(b)

PBEPBE

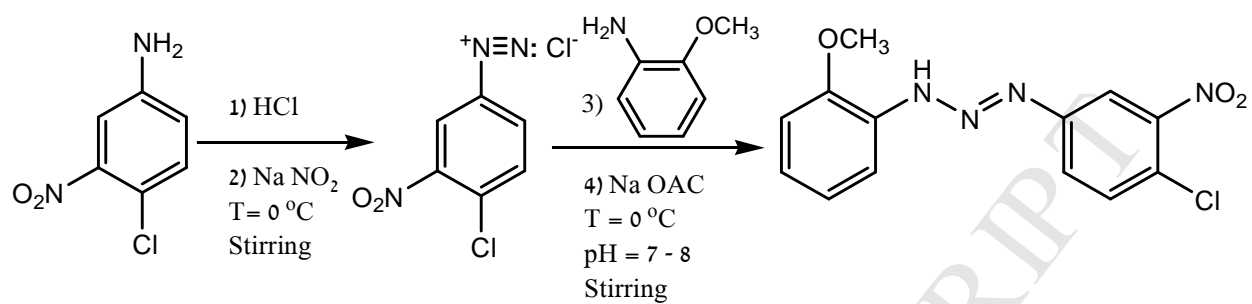
(c)

Fig 4.



Fingerprint plots corresponding Hirshfield surface (Cl atoms: 9.1 %)**Fingerprint plots corresponding Hirshfield surface (H atoms: 51.5 %)****Fingerprint plots corresponding Hirshfield surface (O atoms: 14.3 %)****Fig 5.**

Scheme 1.



Research highlights

- New triazene derivative have been synthesized.
- The structures are determined by X-ray diffraction, NMR and FT-IR spectroscopy.
- All experimental results compared with theoretical study.
- Theoretical results are in good agreement with experimental data.